First-Order Magnetic Raman Scattering from Magnetic-Field Induced Higgs Mode through Second-Order Magnetic Raman Process

Haruhiko KUROE and Tomoyuki SEKINE

Sophia University

Acknowledgements

K. Kusakabe (Sophia Univ.)

Prof. M. Matsumoto (Shizuoka Univ.)

Dr. F. Yamada (TITech)

Dr. A. Oosawa (TITech/Sophia)

Prof. H. Tanaka (TITech)

Contents

1. Rich Physics in $TlCuCl_3$
2. Inelastic Light Scattering [Raman Scattering, (RS)]
3. Experimental Results
4. Discussion
5. Summary

$TlCuCl_3$

Spin Dimer

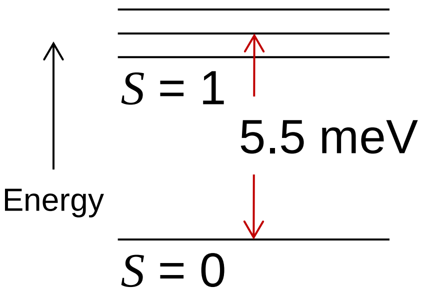

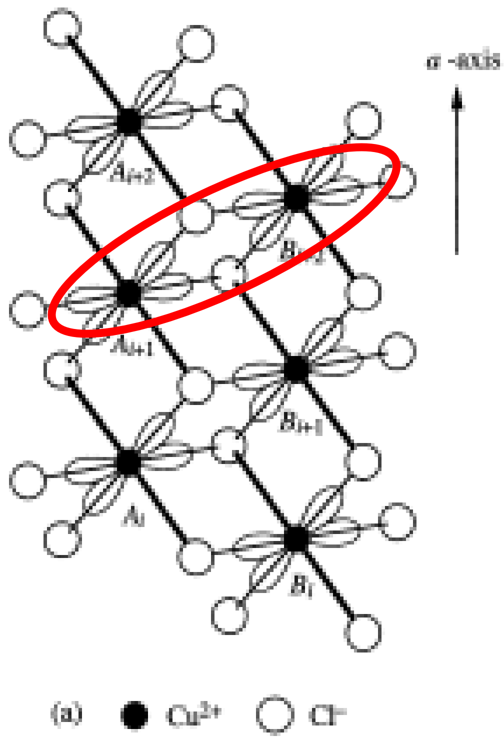

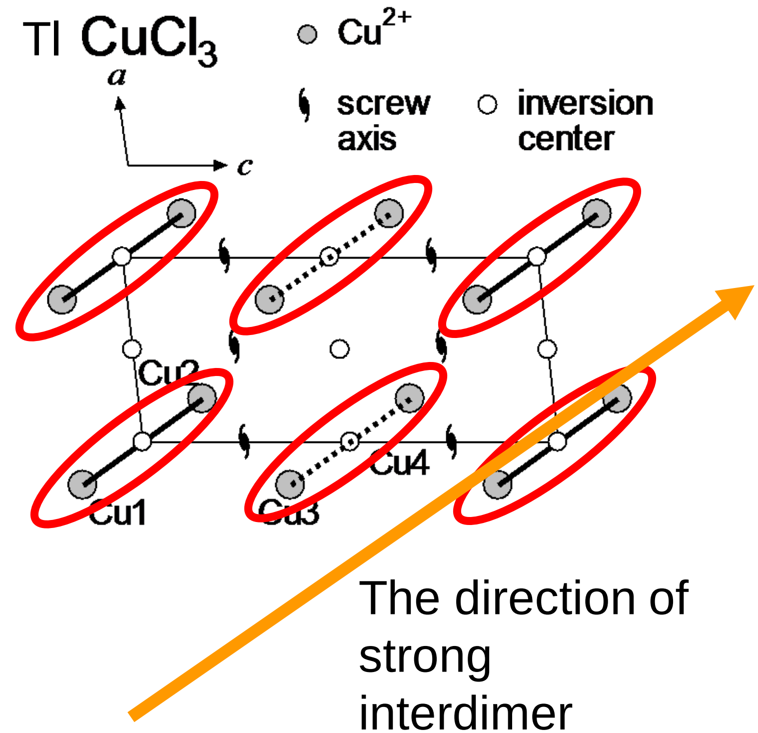

The direction of strong interdimer interaction

[K. Takatsu *et al.*, J. Phys. Soc. Jpn. 66 (1997) 1611.]

Crystal and magnetic structures in $TlCuCl_3$

Magnetic-Field Induced Ordered Phase:
Bose-Einstein Condensation of Magnons

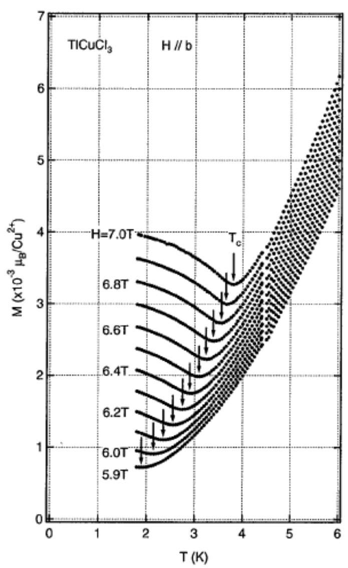

Magnetic-Field induced
Néel order

[A. Oosawa *et al.*, JPCM 11 (1999) 265.]

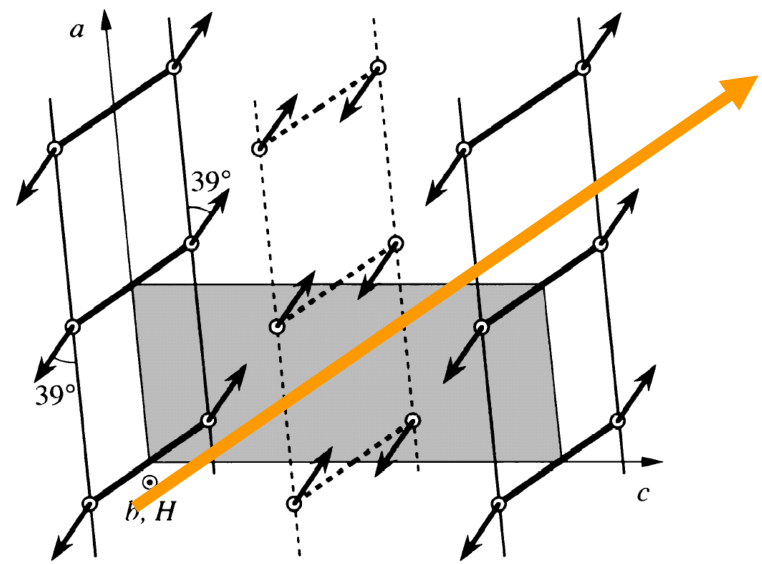

Magnetic structure
under magnetic field

[H. Tanaka *et al.*, JPSJ 70 (2001) 939.]

Pressure Induced Ordered Phase: Pure Higgs Mode

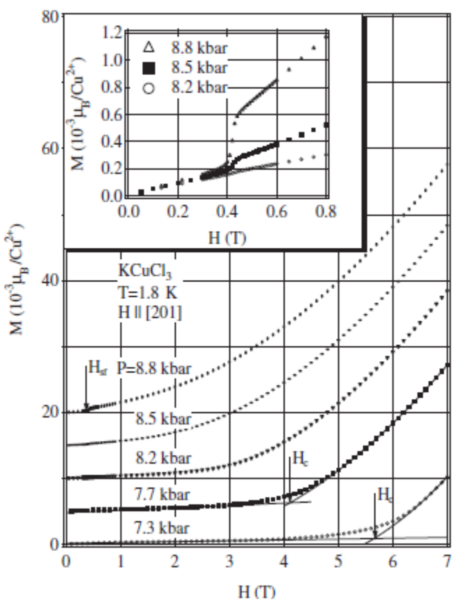

Magnetization

[Goto *et al*., JPSJ 75 (2006) 064703.]

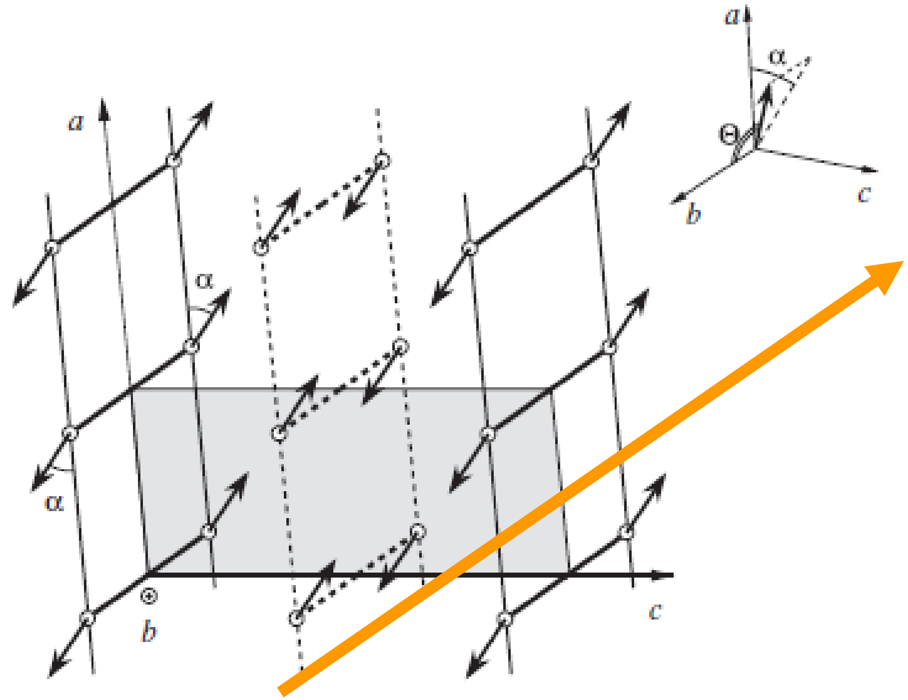

Magnetic structure

[Goto *et al*., JPSJ 75 (2006) 064703.]

Results under high pressures will be available on poster P12.

23/6/2014 @ YITP
Haruhiko KUROE
上智大学 SOPHIA UNIVERSITY

Dispersion Relation: Experiments and Theory

Energy of Spin dimer: 5.5 meV

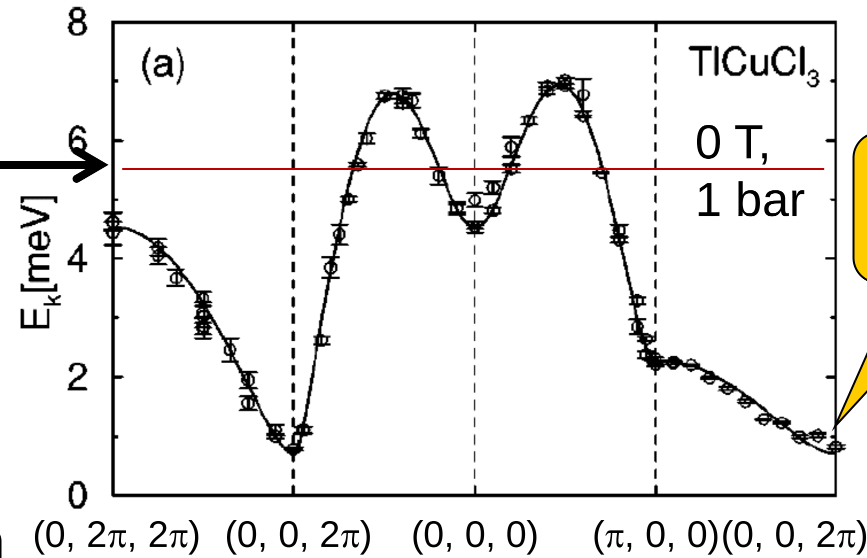

Spin Gap (massive)

!

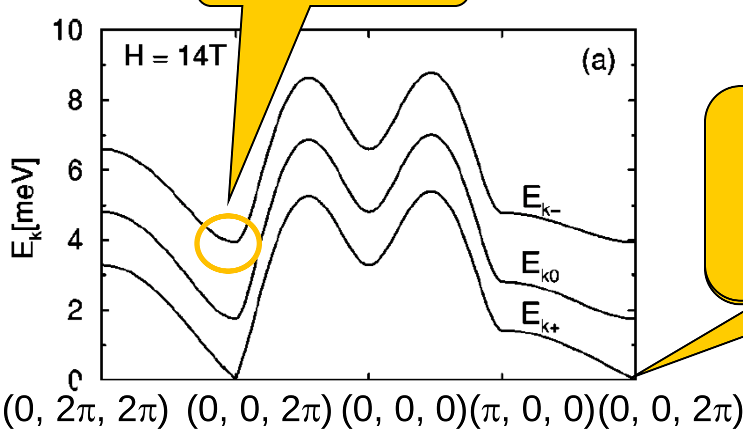

Goldstone Mode (massless)

Higgs Mode (massive)

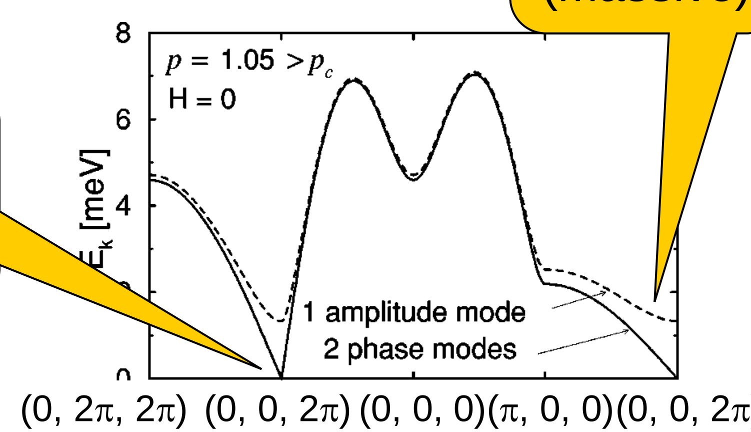

[Experiments: N. Cabadini et al., Phys. Rev. B 63 (2004) 172414.]
[Calculation: M. Matsumoto *et al.*, PRB 69 (2004) 054423.]

Fluctuation of Magnetic Moments

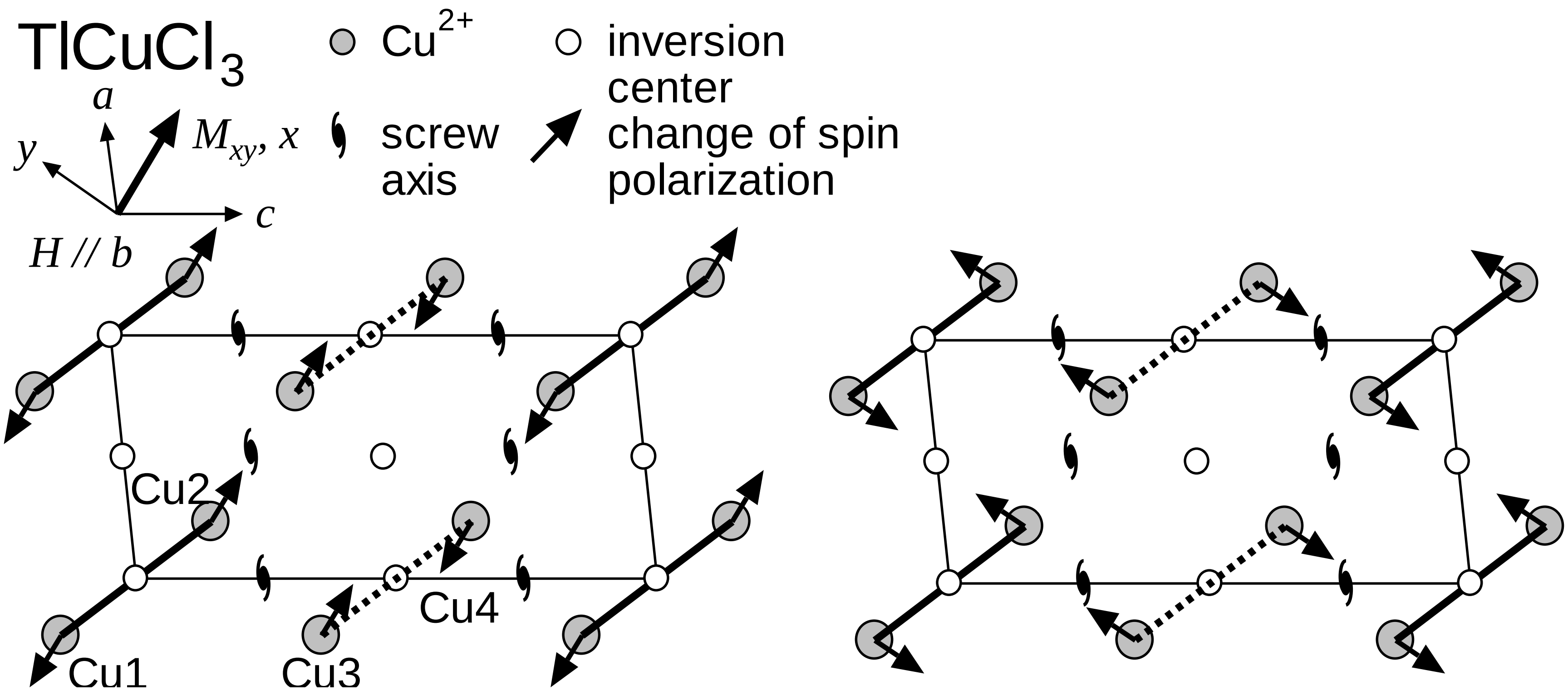

Higgs mode
Amplitude fluctuations

Goldstone mode
Direction fluctuations

Magnon Excitations under Magnetic Field

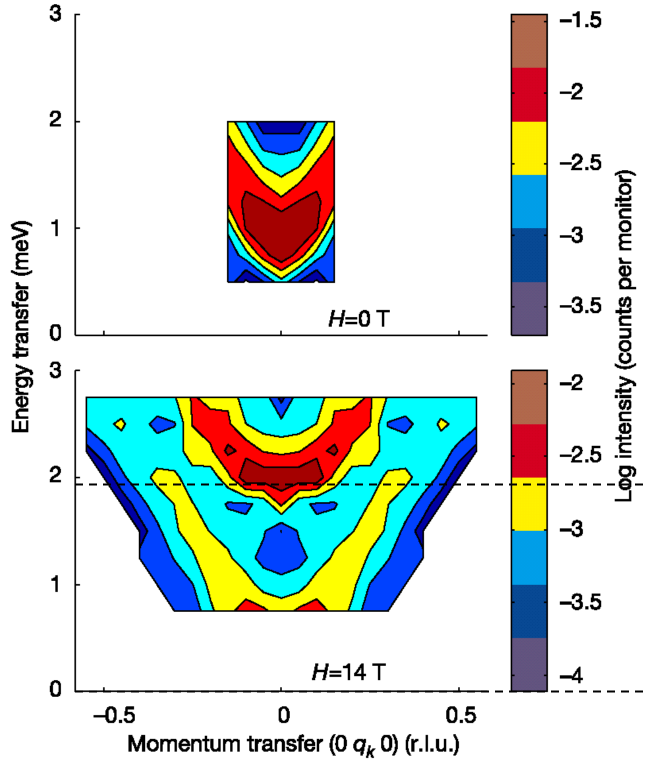

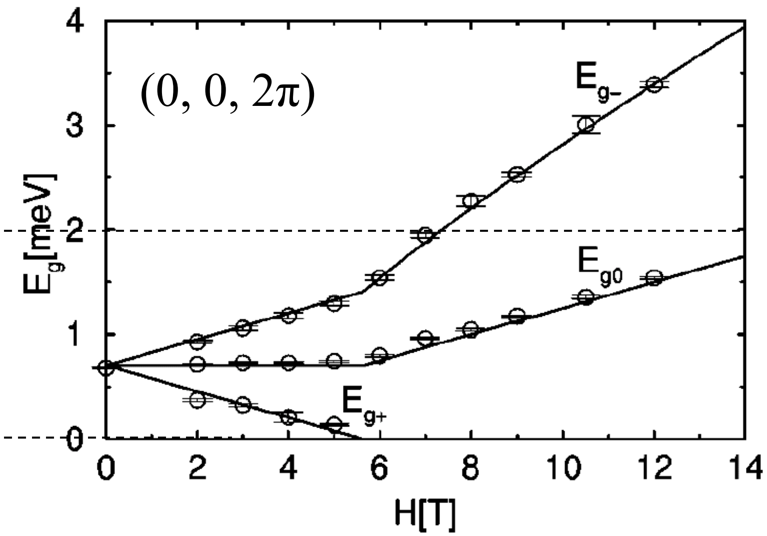

Inelastic neutron scattering in $TlCuCl_3$

[Ch. Rüegg *et al*., Nature 423 (2003) 62.]

Calculation using bond-operator theory

[M. Matsumoto *et al*., PRB 69 (2004) 054423.]

Magnon Excitations under High Pressure

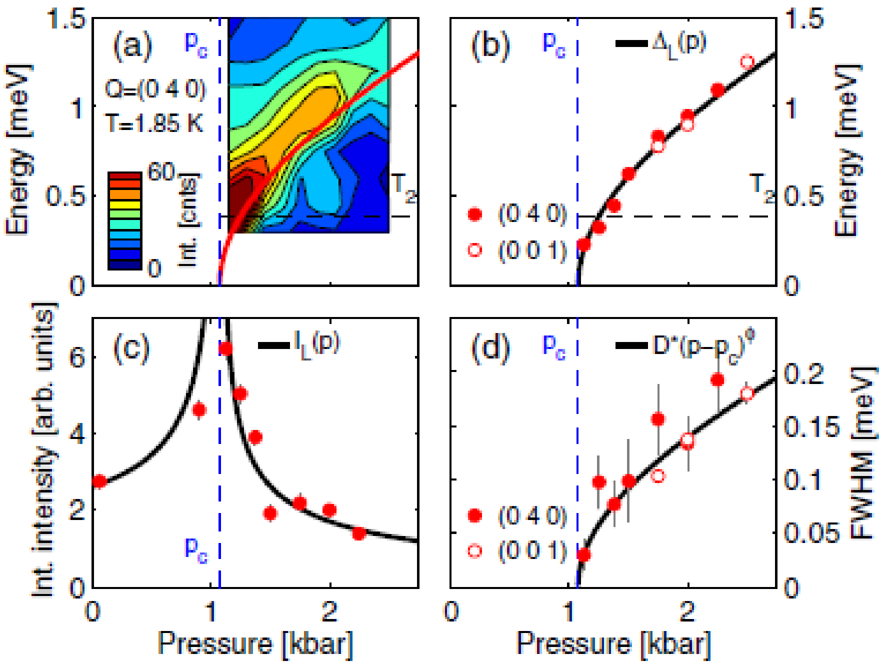

Inelastic neutron scattering in $TlCuCl_3$
[Ch. Rüegg *et al.*, PRL 100 (2008) 205701.]

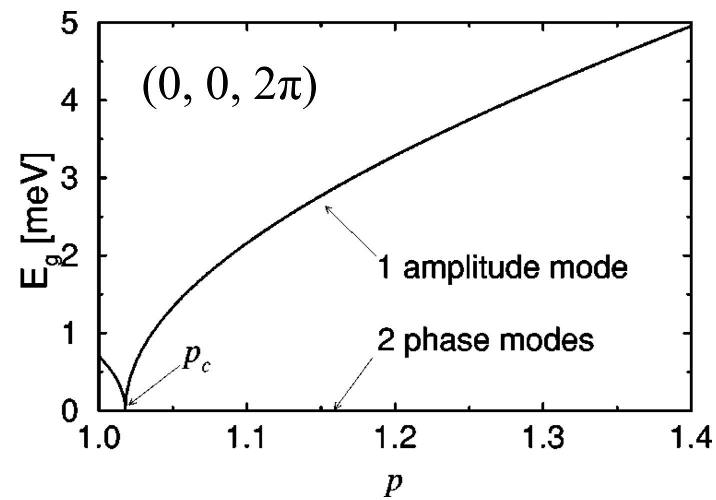

Calculation using bond-operator theory
[M. Matsumoto *et al.*, PRB 69 (2004) 054423.]

Results under high pressures will be available on poster P12.

Latest Topic: Finite-Temperature Effects

nature physics
ARTICLES
PUBLISHED ONLINE: 6 APRIL 2014 | DOI: 10.1038/NPHYS2902

Quantum and classical criticality in a dimerized quantum antiferromagnet

P. Merchant[1], B. Normand[2], K. W. Krämer[3], M. Boehm[4], D. F. McMorrow[1] and Ch. Rüegg[1,5,6*]

A quantum critical point (QCP) is a singularity in the phase diagram arising because of quantum mechanical flu
The exotic properties of some of the most enigmatic physical systems, including unconventional metals and superco
quantum magnets and ultracold atomic condensates, have been related to the importance of critical quantum and
fluctuations near such a point. However, direct and continuous control of these fluctuations has been difficult to re
complete thermodynamic and spectroscopic information is required to disentangle the effects of quantum and classic
around a QCP. Here we achieve this control in a high-pressure, high-resolution neutron scattering experiment on the
dimer material $TlCuCl_3$. By measuring the magnetic excitation spectrum across the entire quantum critical phase
we illustrate the similarities between quantum and thermal melting of magnetic order. We prove the critical nat
unconventional longitudinal (Higgs) mode of the ordered phase by damping it thermally. We demonstrate the devel
two types of criticality, quantum and classical, and use their static and dynamic scaling properties to conclude that
and thermal fluctuations can behave largely independently near a QCP.

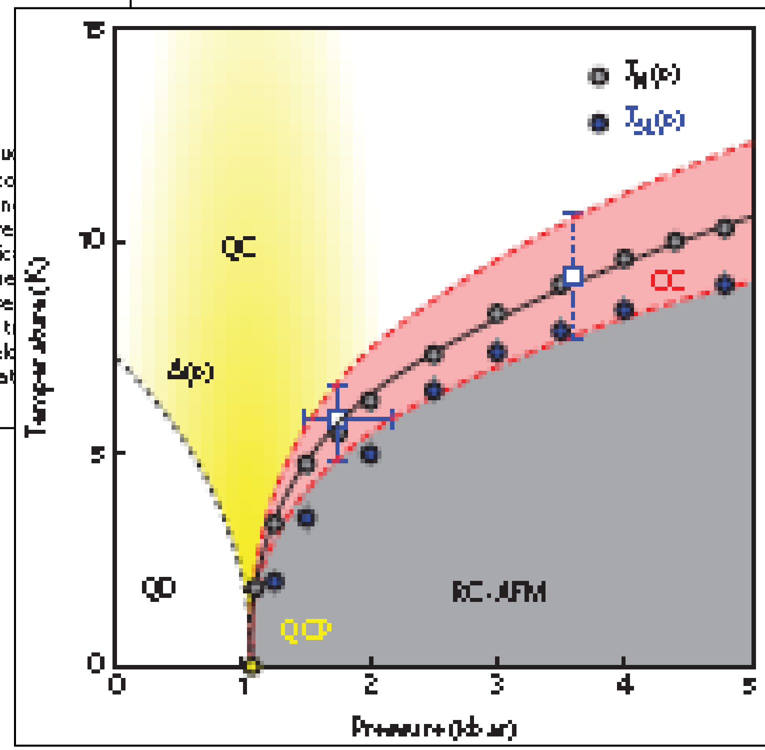

Results under high pressures will be available on poster P12.

Merchant *et al.*, Nature Physics 10 (2014) 373–379.

Contents

Raman Scattering (RS):

- Inelastic light scattering;
- Detection of phonon modes at the chemical Γ point;
- High resolution;
- Symmetry sensitive;
- Small amount of sample;
- Multi-extreme condition; ... and
- Detection of the Higgs mode
  at the magnetic Γ Point !

Contents

1. Rich Physics in ACuCl$_3$ (A = K, Tl)
2. Inelastic Light Scattering [Raman Scattering, (RS)]
3. Experimental Results
4. Discussion
5. Summary

Polarization Characteristics

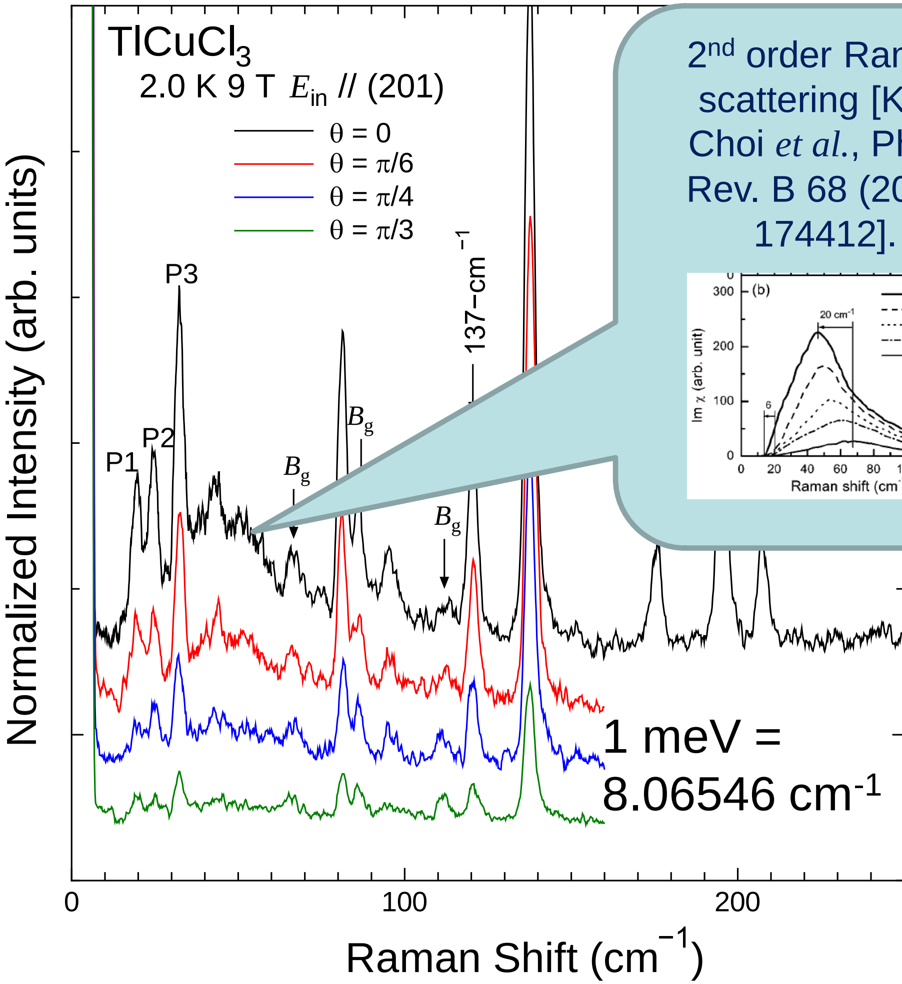

2nd order Raman scattering [K.-Y Choi *et al.*, Phys. Rev. B 68 (2003) 174412].

1 meV = 8.06546 cm^{-1}

Polarized Raman spectra.
P1 mode has the A_g symmetry.

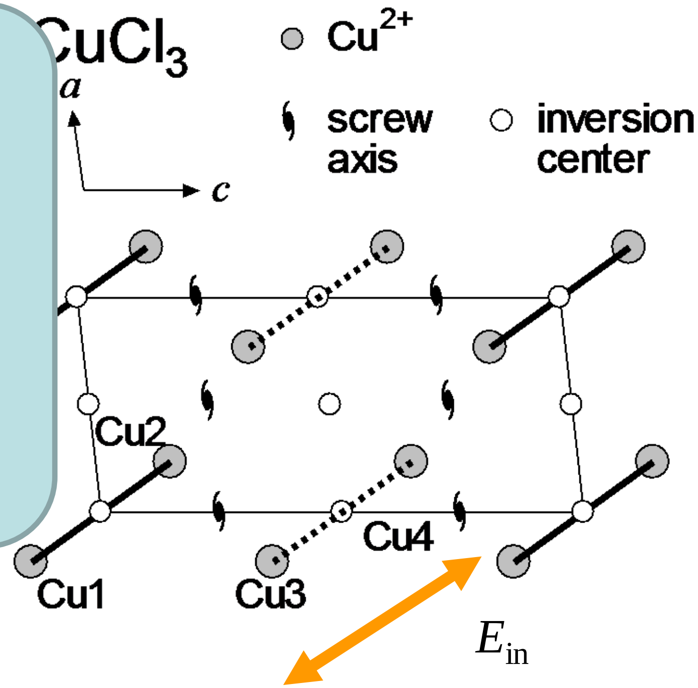

P1 mode was strongly observed for the incident light is polarized along the direction of strong interdimer interaction

Result in $TlCuCl_3$ under Magnetic Field

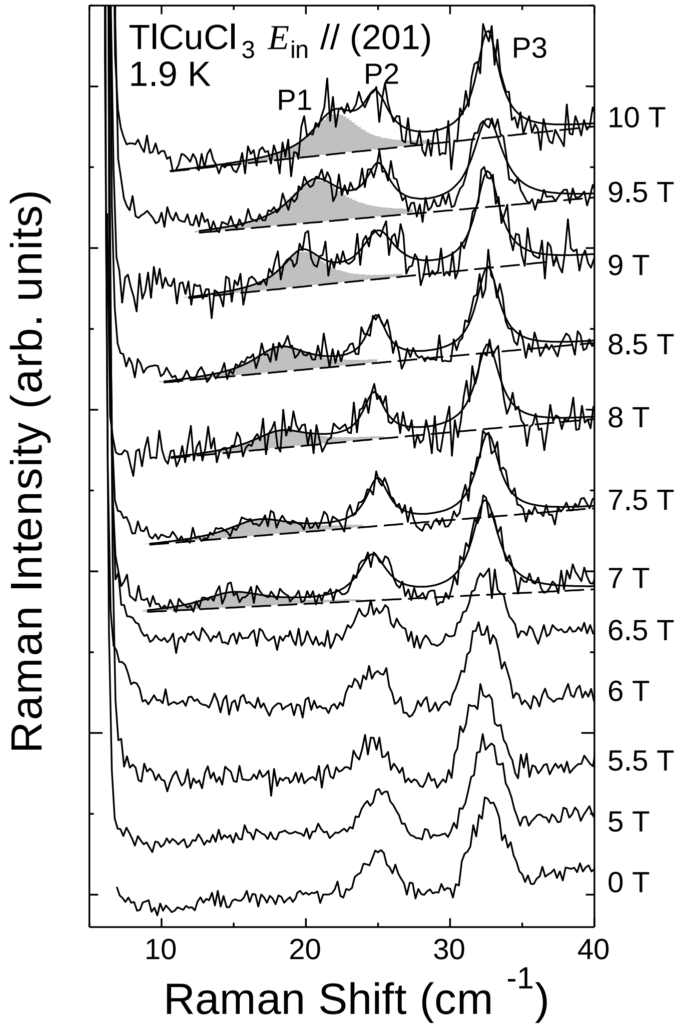

P1 peak is due to the Higgs mode.

Fitting function

$$I = \sum_{1-3} \frac{k_i^2 \omega_i \omega \Gamma_i}{\left(\omega^2 - \omega_i^2\right)^2 + \left(\omega \Gamma_i\right)^2} + (\text{background})$$

$$(\text{background}) = a\omega + b$$

$\hbar\omega_i$ Excitation energy of Pi (i = 1-3)

Γ_i Halfwidth (1/2Γ_i is lifetime)

k_i Coupling coefficient

1 meV = 8.06546 cm^{-1}

H. Kuroe *et al.*, Phys. Rev. B 77 (2008) 134420.

Result in $TlCuCl_3$ under Magnetic Field

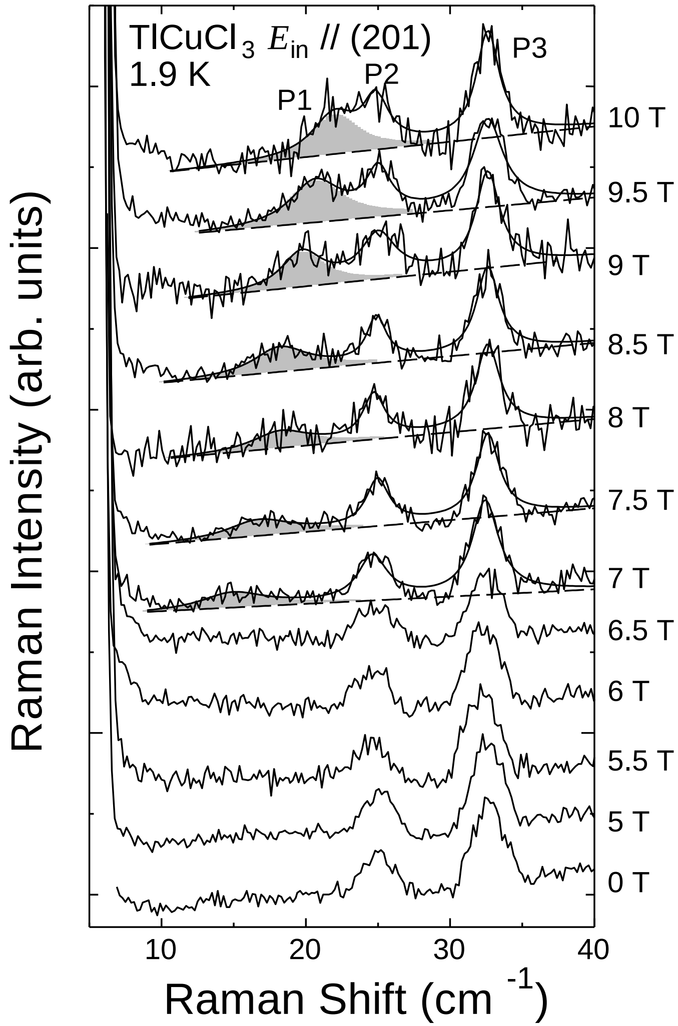

P1 peak is due to the Higgs mode.

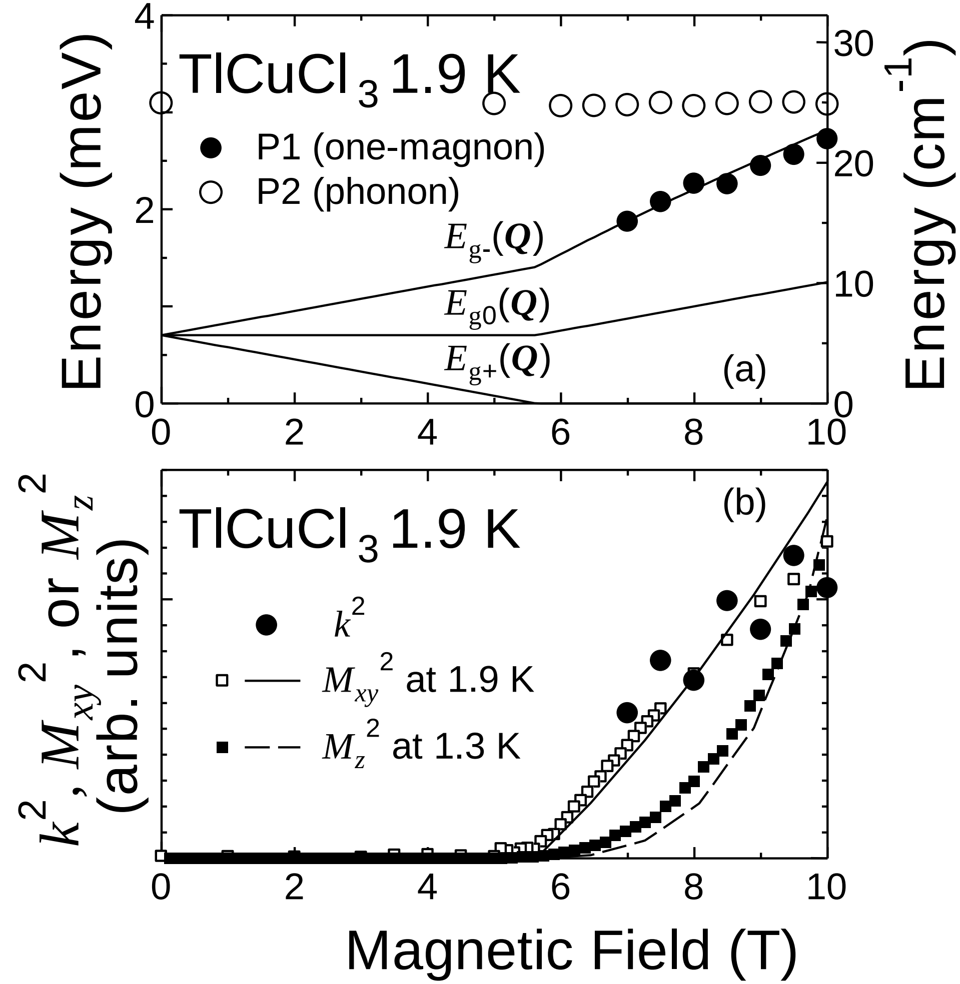

Magnetic field dependences of P1 energy (upper panel) and integrated intensity (lower panel).

Summary of Experimental Results:

- We observe strong magnetic RS when the incident light is polarized along the direction of strong interdimer interaction;
- 1st Order magnetic RS never appears below H_c or below p_c;
- Raman intensity is proportional to M_{xy}^2;
- Energy of the P1 peak is well described by the energy of the Higgs mode;
- Halfwidth of the P1 peak under high pressures is proportional to the P1-peak energy.

We should understand these facts theoretically to clarify the fact that

Magnetic RS detects the Higgs mode.

Contents

1. Rich Physics in $A\mathrm{CuCl}_3$ (A = K, Tl)
2. Inelastic Light Scattering [Raman Scattering, (RS)]
3. Experimental Results
4. Discussion
5. Summary

Second-order magnetic RS: Optically Induced Spin Exchange

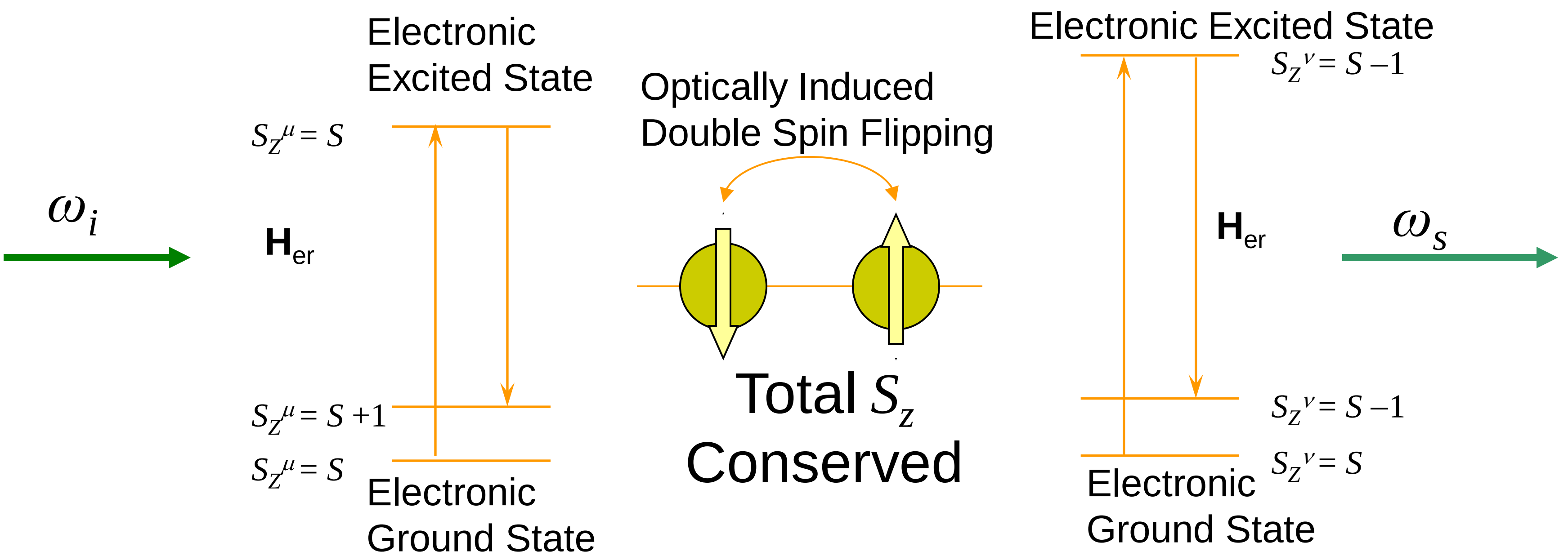

P. A. Fleury and R. Loudon , Phys. Rev. 166 (1968) 514.

Effective Raman operator $$R = \sum_{i,j} F_{i,j}\left(\hat{E}_{\text{in}}\cdot\hat{r}_{i,j}\right)\left(\hat{E}_{\text{sc}}\cdot\hat{r}_{i,j}\right)\vec{S}_i\cdot\vec{S}_j$$

$\vec{S}_i$ S = 1/2 Spin at site i

$\hat{r}_{i,j}$ Unit vector connecting sites i, j

$\hat{E}_{\text{in(sc)}}$ Polarization of incident (scattered) light

$F_{i,j}$ Amplitude factor

Summary of Experimental Results:

- ☑ We observe strong magnetic RS when the incident light is polarized along the direction of strong interdimer interaction;
- ☐ 1st Order magnetic RS never appears below H_c or below p_c;
- ☐ Raman intensity is proportional to M_{xy}^2;
- ☐ Energy of the P1 peak is the same as that of the Higgs mode;
- ☐ Halfwidth of the P1 peak under high pressures is proportional to the P1-peak energy.

We should understand these facts theoretically to clarify the fact that

Magnetic RS detects the Higgs mode.

The Toy

Two S = ½ Spin dimers with degrees of freedom (DoF) $2^4 = 16$

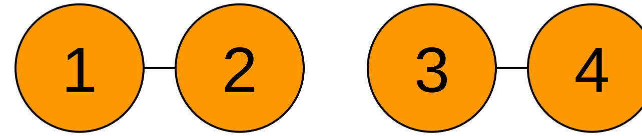

Singlet sate (DoF 1)

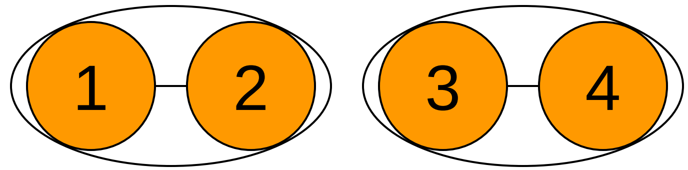

$|\sigma\sigma\rangle$

One magnon state (DoF 6)

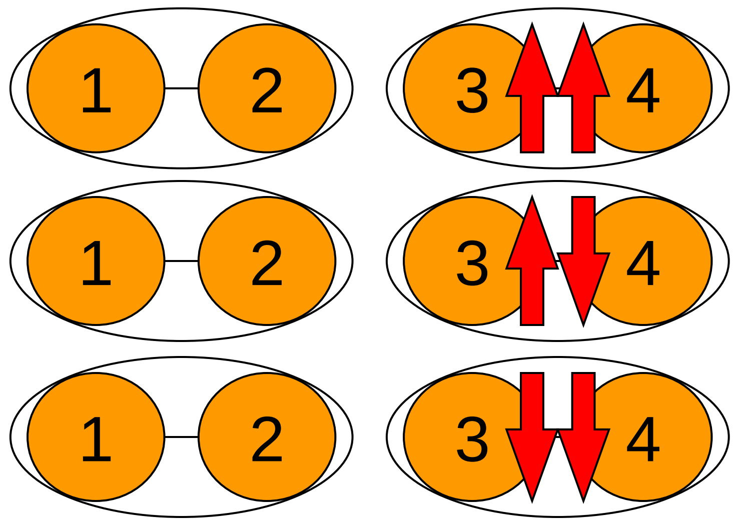

$|\sigma\tau_{+}\rangle$

$|\sigma\tau_{0}\rangle$

$|\sigma\tau_{-}\rangle$

…

Two magnon state (DoF 9)

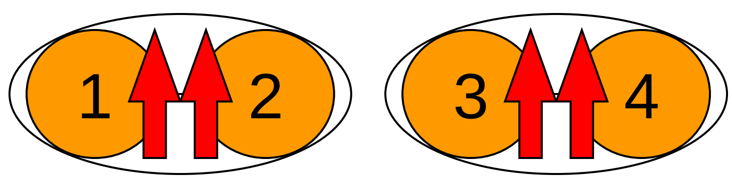

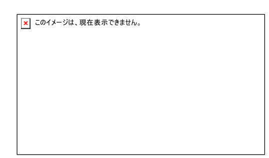

…

Operate Effective Raman Operator

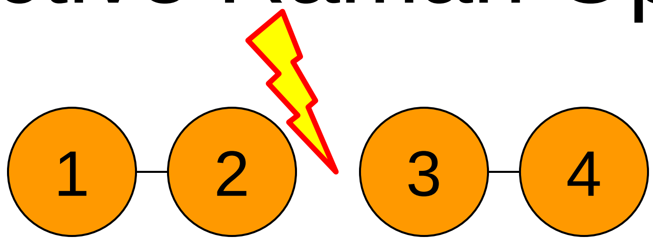

$$\tilde{R}\left|\sigma\sigma\right\rangle = \vec{S}_2 \cdot \vec{S}_3 \left|\sigma\sigma\right\rangle$$

$$= \left\{ \frac{S_2^+ S_3^- + S_2^- S_3^+}{2} + S_2^z S_3^z \right\} \left\{ \frac{\left|\uparrow\downarrow\uparrow\downarrow\right\rangle - \left|\downarrow\uparrow\uparrow\downarrow\right\rangle - \left|\uparrow\downarrow\downarrow\uparrow\right\rangle + \left|\downarrow\uparrow\downarrow\uparrow\right\rangle}{2} \right\}$$

$$= \left\{ \frac{\left|\uparrow\uparrow\downarrow\downarrow\right\rangle + \left|\downarrow\downarrow\uparrow\uparrow\right\rangle}{4} \right\} + \frac{1}{4} \left\{ \frac{-\left|\uparrow\downarrow\uparrow\downarrow\right\rangle - \left|\downarrow\uparrow\uparrow\downarrow\right\rangle - \left|\uparrow\downarrow\downarrow\uparrow\right\rangle - \left|\downarrow\uparrow\downarrow\uparrow\right\rangle}{2} \right\}$$

$$= \frac{1}{4}\left(\left|\tau_+\tau_-\right\rangle + \left|\tau_-\tau_+\right\rangle - \left|\tau_0\tau_0\right\rangle \right)$$

Excitation between singlet state to two magnon state;

Conservation of angular momentum

$$\tilde{R}\left|\sigma\tau_+\right\rangle = \vec{S}_2\cdot\vec{S}_3\left|\sigma\tau_+\right\rangle$$

$$= \left\{\frac{S_2^+S_3^- + S_2^-S_3^+}{2} + S_2^zS_3^z\right\}\left\{\frac{\left|\uparrow\downarrow\uparrow\uparrow\right\rangle - \left|\downarrow\uparrow\uparrow\uparrow\right\rangle}{\sqrt{2}}\right\}$$

$$= \frac{S_2^+S_3^- + S_2^-S_3^+}{2}\left\{\frac{\left|\uparrow\downarrow\uparrow\uparrow\right\rangle - \left|\downarrow\uparrow\uparrow\uparrow\right\rangle}{\sqrt{2}}\right\} + S_2^zS_3^z\left\{\frac{\left|\uparrow\downarrow\uparrow\uparrow\right\rangle - \left|\downarrow\uparrow\uparrow\uparrow\right\rangle}{\sqrt{2}}\right\}$$

$$= \frac{\left|\uparrow\uparrow\downarrow\uparrow\right\rangle}{2\sqrt{2}} + \frac{1}{4}\left\{\frac{-\left|\uparrow\downarrow\uparrow\uparrow\right\rangle - \left|\downarrow\uparrow\uparrow\uparrow\right\rangle}{\sqrt{2}}\right\}$$

$$= \frac{1}{4}\frac{\left|\uparrow\uparrow\downarrow\uparrow\right\rangle - \left|\uparrow\uparrow\uparrow\downarrow\right\rangle}{\sqrt{2}} + \frac{1}{4}\frac{\left|\uparrow\uparrow\downarrow\uparrow\right\rangle + \left|\uparrow\uparrow\uparrow\downarrow\right\rangle}{\sqrt{2}} - \frac{1}{4}\frac{\left|\uparrow\downarrow\uparrow\uparrow\right\rangle + \left|\downarrow\uparrow\uparrow\uparrow\right\rangle}{\sqrt{2}}$$

$$= \frac{1}{4}\left|\tau_+\sigma\right\rangle + \frac{1}{4}\left|\tau_+\tau_0\right\rangle - \frac{1}{4}\left|\tau_0\tau_+\right\rangle$$

Excitation between <u>one magnon state to two magnon state</u>;

Conservation of angular momentum

Summary of Experimental Results:

- ☑ We observe strong magnetic RS when the incident light is polarized along the direction of strong interdimer interaction;
- ☑ 1st order magnetic RS never appears below H_c or below p_c;
- ☐ Raman intensity is proportional to M_{xy}^2;
- ☐ Energy of the P1 peak is the same as that of the Higgs mode;
- ☐ Halfwidth of the P1 peak under high pressures is proportional to the P1-peak energy.

We should understand these facts theoretically to clarify the fact that

Magnetic RS detects the Higgs mode.

Singlet-triplet mixing under magnetic field

M. Matsumoto *et al*., PRB 69 (2004) 054423.

In ordered phase ($H_c < H < H_s$)

$$a_i = us_i + v(fe^{iQ\cdot r_i}t_{i+} + ge^{iQ\cdot r_i}t_{i-}),$$

$$b_{i+} = u(ft_{i+} + gt_{i-}) - ve^{iQ\cdot r_i}s_i,$$

$$b_{i0} = t_{i0},$$

$$b_{i-} = ft_{i-} - gt_{i+},$$

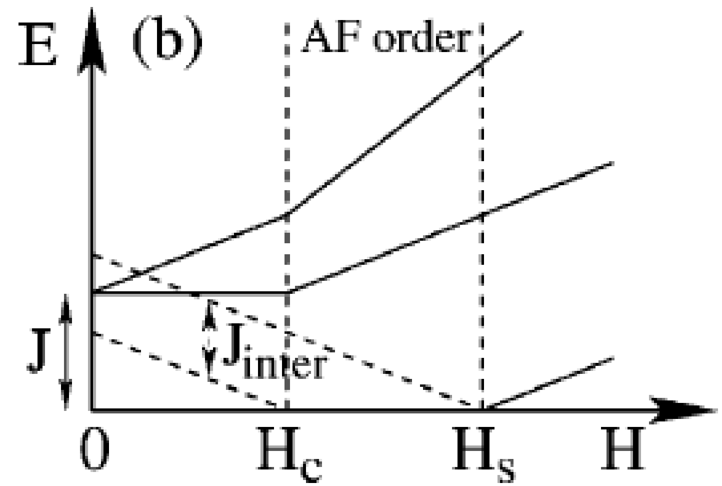

Magnetic RS detects singlet-triplet mixing

Writing effective Raman operator using s_i and $t_{i\alpha}$

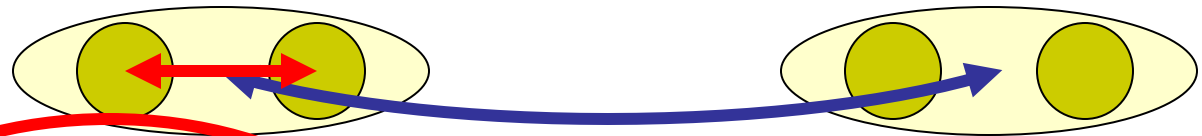

Intradimer part

$$R_{\text{intra}} = F_{\text{intra}}\left(\hat{E}_{\text{in}}\cdot\hat{d}\right)\left(\hat{E}_{\text{sc}}\cdot\hat{d}\right) \times \sum_i \left(-\frac{3}{4}s_i^\dagger s_i + \sum_{\alpha=0,\pm}\frac{1}{4}t_{i\alpha}^\dagger t_{i\alpha}\right)$$

Interdimer part

$$R_{\text{inter}} = F_{\text{inter}}\left(\hat{E}_{\text{in}}\cdot\hat{R}_{ij}\right)\left(\hat{E}_{\text{sc}}\cdot\hat{R}_{ij}\right) \times \sum_{ij}\left\{\left[t_{i\alpha}^\dagger t_{j\alpha} s_j^\dagger s_i + t_{i\alpha}^\dagger t_{j\bar{\alpha}}^\dagger s_i s_j + \text{H.c.}\right] + \left[t_{i0}^\dagger t_{j0}\left(t_{i+}^\dagger t_{j+} + t_{i-}^\dagger t_{j-}\right) + \text{H.c.}\right] - \left[t_{i0} t_{j0}\left(t_{i+}^\dagger t_{j-}^\dagger + t_{i-}^\dagger t_{j+}^\dagger\right) + \text{H.c.}\right] + \left(t_{i+}^\dagger t_{i+} - t_{i-}^\dagger t_{i-}\right)\left(t_{j+}^\dagger t_{j+} - t_{j-}^\dagger t_{j-}\right)\right\}$$

Writing the singlet-triplet mixing in the ***k*** space

Matsumoto *et al.*,
PRL 89, 077203 (2002),
PRB 69, 054423 (2004).

$s_{\boldsymbol{k}},\ t_{\boldsymbol{k}+}\ t_{\boldsymbol{k}0}\ t_{\boldsymbol{k}-}$

↓

$a_k, b_{k+}, b_{k0}, b_{k-}$

$$a_k = us_k + vft_{k+Q+} + vgt_{k+Q-}$$
$$b_{k+} = -vs_{k+Q} + uft_{k+} + ugt_{k-}$$
$$b_{k-} = ft_{k-} - gt_{k+}$$
$$b_{k0} = t_{k0}$$

The magnetic Γ point

Writing effective Raman operator with the basis of $b_{k0},\ b_{k\pm}$:

$$R_{\text{intra}} = F_{\text{intra}}\left(\hat{E}_{\text{in}}\cdot\hat{d}\right)\left(\hat{E}_{\text{sc}}\cdot\hat{d}\right)\sum_k\left(-\frac{3}{4}s_k^\dagger s_k + \sum_{\alpha=0,\pm}\frac{1}{4}t_{k\alpha}^\dagger t_{k\alpha}\right)$$

$$= F_{\text{intra}}\left(\hat{E}_{\text{in}}\cdot\hat{d}\right)\left(\hat{E}_{\text{sc}}\cdot\hat{d}\right)\left[\left(\frac{1}{4}-u^2\right)\bar{a}^2 + \underline{uv\bar{a}\left(b_{Q+}^\dagger + b_{Q+}\right)} + \sum_k\left\{\left(\frac{1}{4}-v^2\right)b_{k+}^\dagger b_{k+} + \frac{1}{4}b_{k-}^\dagger b_{k-} + \frac{1}{4}b_{k0}^\dagger b_{k0}\right\}\right]$$

$$uv \propto M_{xy}$$

$$I = \frac{2\pi}{\hbar}\left|\left\langle f\left|R_{\text{intra}}\right|i\right\rangle\right|^2$$

1st order magnetic RS Is observed in the second-order Raman process:

1. above H_c;
2. at the Γ point;
3. with the intensity proportional to M_{xy}^2.

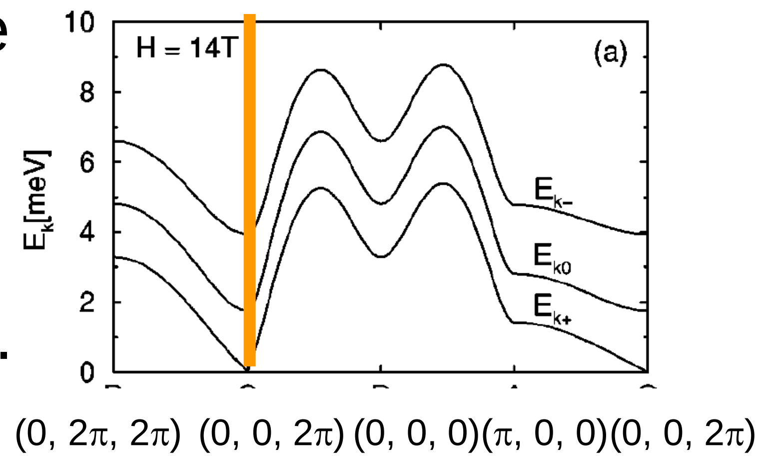

Summary of Experimental Results:

- ☑ We observe strong magnetic RS when the incident light is polarized along the direction of strong interdimer interaction;
- ☑ 1st order magnetic RS never appears below H_c or below p_c;
- ☑ Raman intensity is proportional to M_{xy}^2;
- ☐ Energy of the P1 peak is the same as that of the Higgs mode;
- ☐ Halfwidth of the P1 peak under high pressures is proportional to the P1-peak energy.

We should understand these facts theoretically to clarify the fact that

Magnetic RS detects the Higgs mode.

Diagonalization to calculate scattering intensity

Matsumoto *et al.*,
PRL 89, 077203 (2002),
PRB 69, 054423 (2004).

$$
\begin{aligned}
a_k &= u s_k + v f t_{k+Q+} + v g t_{k+Q-} \\
b_{k+} &= -v s_{k+Q} + u f t_{k+} + u g t_{k-} \\
b_{k-} &= f t_{k-} - g t_{k+} \\
b_{k0} &= t_{k0}
\end{aligned}
$$

$$s_{\mathbf{k}},\ t_{\mathbf{k}+}\ \ t_{\mathbf{k}0}\ \ t_{\mathbf{k}-}$$

↓

$$a_k,\ b_{k+},\ b_{k0},\ b_{k-}$$

↓

$$a_k,\ \alpha_k^{+},\ \alpha_k^{0},\ \alpha_k^{-}$$

Bogoliubov Transformation

$$
\begin{pmatrix} \alpha_k^- \\ \alpha_k^+ \\ \alpha_k^{-\dagger} \\ \alpha_k^{+\dagger} \end{pmatrix}
=
\begin{pmatrix}
u_{k-}^- & u_{k+}^- & v_{k-}^- & v_{k+}^- \\
u_{k-}^+ & u_{k+}^+ & v_{k-}^+ & v_{k+}^+ \\
v_{-k-}^- & v_{-k+}^- & u_{-k-}^- & u_{-k+}^- \\
v_{-k-}^+ & v_{-k+}^+ & u_{-k-}^+ & u_{-k+}^+
\end{pmatrix}
\begin{pmatrix} b_{k-} \\ b_{k+} \\ b_{-k-}^\dagger \\ b_{-k+}^\dagger \end{pmatrix}
$$

For Higgs and Goldstone Modes, we have

$$
b_{Q+} + b_{Q+}^\dagger = \left(u_{Q+}^- - v_{Q+}^-\right)^* \alpha_Q^- + \left(u_{Q+}^- - v_{Q+}^-\right)\alpha_Q^{-\dagger}
$$

$$
\underbrace{+\left(u_{Q+}^+ - v_{Q+}^+\right)^* \alpha_Q^+ + \left(u_{Q+}^+ - v_{Q+}^+\right)\alpha_Q^{+\dagger}}_{\text{zero}}
$$

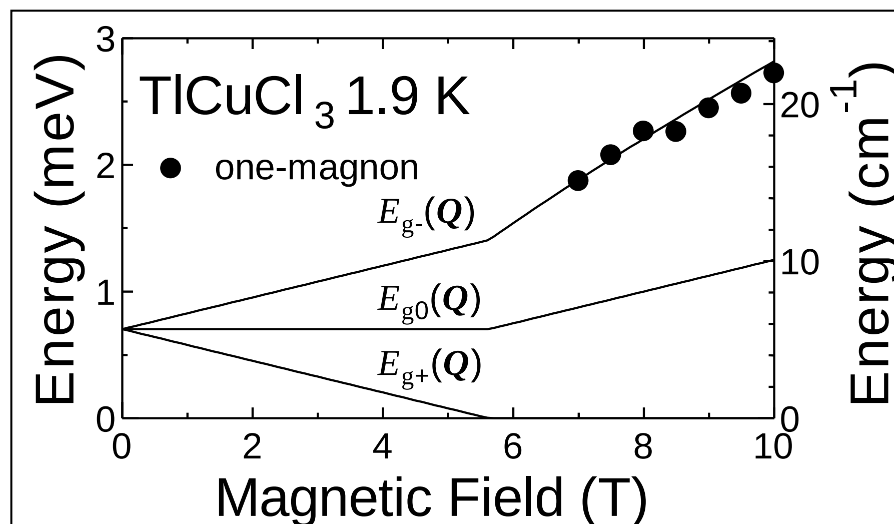

Summary of Experimental Results:

- ☑ We observe strong magnetic RS when the incident light is polarized along the direction of strong interdimer interaction;
- ☑ 1st order magnetic RS never appears below H_c or below p_c;
- ☑ Raman intensity is proportional to $M_{xy}{}^2$;
- ☑ Energy of the P1 peak is the same as that of the Higgs mode;
- ☐ Halfwidth of the P1 peak under high pressures is proportional to the P1-peak energy.

We should understand these facts theoretically to clarify the fact that

Magnetic RS detects the Higgs mode.

Contents

Summary of Experimental Results and Theoretical Consideration:

- ☑ We observe strong magnetic RS when the incident light is polarized along the direction of strong interdimer interaction;
- ☑ 1st Order magnetic RS never appears below H_c or below p_c;
- ☑ Raman intensity is proportional to M_{xy}^2;
- ☑ Energy of the P1 peak is the same as that of the Higgs mode;
- ☑ Halfwidth of the P1 peak under high pressures is proportional to the P1-peak energy.

We conclude that

Magnetic RS detects the Higgs mode.